Progressive decrease of mitochondrial motility during maturation of cortical axons *in vitro* and *in vivo*

Tommy L. Lewis Jr., **Gergely F. Turi**, **Seok-Kyu Kwon**, **Attila Losonczy**, and **Franck Polleux**[*]

Columbia University Medical Center - Department of Neuroscience, Mortimer B. Zuckerman Mind Brain Behavior Institute, Kavli Institute for Brain Science 550 West 120th Street, 1103 NWC Building, New York, NY 10027

Summary

The importance of mitochondria for neuronal function is evident by the large number of neurodegenerative diseases which have been associated with a disruption of mitochondrial function or transport (reviewed in [1, 2]). Mitochondria are essential for proper biological function as a result of their ability to produce ATP through oxidative phosphorylation, buffer cytoplasmic calcium, regulate lipid biosynthesis and trigger apoptosis (reviewed in [2]). Efficient transport of mitochondria is thought to be particularly important in neurons in light of their compartmentalization, length of axonal processes and high-energy requirements (reviewed in [3]). However, the majority of these results were obtained using short-term, *in vitro* neuronal culture models and very little is currently known about mitochondrial dynamics in mature axons of the mammalian central nervous system (CNS) *in vitro* or *in vivo*. Furthermore, recent evidence has demonstrated that mitochondrial immobilization at specific points along the axon, such as presynaptic boutons, play critical roles in axon morphogenesis [4, 5]. We report that as cortical axons mature, motility of mitochondria (but not other cargoes) is dramatically reduced and this coincides with increased localization to presynaptic sites. We also demonstrate, using photo-conversion, that *in vitro* mature axons display surprisingly limited long-range mitochondrial transport. Finally, using *in vivo* 2-photon microscopy in anesthetized or awake behaving mice, we document for the first time that mitochondrial motility is also remarkably low in distal cortical axons *in vivo*. These results argue that mitochondrial immobilization and presynaptic localization are important hallmarks of mature CNS axons both *in vitro* and *in vivo*.

Results and Discussion

Mitochondrial motility decreases progressively with axonal maturation and coincides with increased presynaptic localization *in vitro*

To better understand mitochondrial localization at presynaptic sites, we performed live dual-channel time-lapse imaging of mitochondria and VGLUT1-labeled presynaptic boutons following *ex utero* cortical electroporation, dissociation and primary neuronal culture. As previously observed, early stages (3–7DIV) of axonal development display a substantial fraction of highly motile mitochondria (Figure 1A–B) [4, 6, 7]. However as the axon matured (10DIV), mitochondria became less motile (Figure 1C–F, G,I). By 28DIV, more than 95% of axonal mitochondria were stationary over the 30 minutes of imaging compared to approximately 60% at 7DIV (ANOVA, p<0.0001). This decrease in mitochondrial motility coincides with the formation of stable *en passant* VGLUT1-positive presynaptic sites along the axon (Figure 1B–F, Movie S1). Stable presynaptic boutons begin to appear around 7DIV thus we quantified the percent of stationary mitochondria localized at stable presynaptic sites for the entire 30 minutes of imaging (Figure 1H,I), and found that early in axonal development (7DIV) approximately 20% of stationary mitochondria are localized at presynaptic sites. This percentage steadily increases with development until approximately half of all axonal mitochondria are localized at presynaptic boutons (Figure 1H, ANOVA, p<0.0001). Interestingly, this represents a substantial increase in presynaptic localization when one considers that approximately 40% of mitochondria at 7DIV are not included in this quantification as they are not stationary. Our data so far suggests a model whereby mitochondrial motility is significantly lower in mature axons than previously proposed from the results obtained in immature, developing axons of dissociated cultured neurons (usually 5–7DIV; e.g. [8, 9]). In the present report and another recent study in hippocampal neurons [10], mitochondria are shown to be considerably more stable in mature axons (14DIV) than in immature axons *in vitro*. These reports also demonstrate that mitochondrial immobilization correlates with their localization to presynaptic boutons along CNS axons (Table S1). Together these results reveal that mitochondrial motility decreases with axonal maturation partially as a result of presynaptic immobilization. In the future, it will be important to better understand the cellular and molecular mechanisms which regulate long-term immobilization of mitochondria, the role of mitochondria localized at presynaptic sites versus other sites along the axon, as well as the effects that presynaptically localized mitochondria exert on presynaptic release properties.

Lysosomal motility is not affected by axonal maturation *in vitro*

To determine if the decrease in mitochondrial motility is specific to this cargo or if cargo trafficking in general is lower in mature axons, we performed live dual-channel time-lapse imaging of LAMP1-labeled lysosomes and mitochondria in immature (7DIV) and mature (28DIV) axons (Figure 2A–F, Movie S2). We chose lysosomes as a cargo because recent evidence suggested that axonal mitochondria are locally engaged by autophagosomes fusing to lysosomes for removal by local mitophagy [11, 12]. While the fraction of stationary mitochondria increases from around 65% to ~98% between 7DIV and 28DIV, the percentage of stationary lysosomes did not change significantly (Figure 2G, ANOVA, p<0.05 for mitochondria, no significance for lysosomes). While the number of motile versus

stationary lysosomes was not changed, there was a decrease in the velocity of the lysosomes and a small increase in retrograde run time in mature axons (Figure 2H, ANOVA, p<0.001 for velocity, p<0.05 for retrograde run time). The observation that the fraction of motile lysosomes is unchanged in mature axons is consistent with recent work demonstrating that autophagosomes need to be transported back to the cell body to undergo fusion with lysosomes [13], and suggests that the decrease in mitochondrial motility in mature axons *in vitro* is rather specific to this organelle.

Mitochondria in mature axons are functional

One possible explanation for the decrease in mitochondrial motility observed in late stage cultures could be that mitochondrial function is compromised. To measure the functionality of mitochondria under these conditions, we imaged mitochondrial membrane potential via tetramethylrhodamine (TMRM, [14]) and mitochondrial matrix calcium dynamics during action potential (AP) evoked neurotransmitter release using a genetically-encoded, matrix-targeted calcium indicator GCaMP5G (mito-GCaMP5G) [15]. Mitochondrial membrane potential is generated via the proton gradient, resulting from oxidative phosphorylation along the electron transport chain (ETC), across the inner mitochondrial membrane (IMM) which gates ATP generation. We observed that mitochondria in the axon of neurons cultured for 7DIV or 28DIV effectively took up TMRM and determined that there was no difference in the ratio of mitochondrial fluorescence to cytoplasmic fluorescence (Fm/Fc, [14]) (Figure S1A–B). This result establishes that mitochondria do not display significant changes in their membrane potential during axon maturation *in vitro*. To test whether or not mitochondria are capable of importing calcium during AP-evoked release [16], we applied 100APs at 10Hz using a micropipette stimulation near the labeled axons and found that mitochondria in both immature and mature axons responded by importing calcium into their matrix on similar timescales (Figure S1D–G). We calculated the area under the curves (as an estimate of the 'total charge transfer') and found a small but significant increase in the amount of calcium imported by mitochondria in mature axons *in vitro* (Supplemental Figure 1G). We also observed an increase in the basal level of calcium in the matrix of mitochondria in mature axons compared to immature axons (Supplemental Figure 1E). It is likely that increased neuronal activity, mediated by mature synapses, in these older cultures is at least partially responsible for both the increased basal level of calcium in the mitochondrial matrix and the increase in calcium that is imported upon stimulation. This increase in AP-evoked mitochondrial calcium import in mature axons might be linked to decreased mitochondrial motility although the mechanisms by which intramitochondrial calcium regulate mitochondrial trafficking remain controversial [8, 17–19].

Long-term timelapse microscopy reveals that mitochondria in mature axons remain stable over an extended period of time

To determine the stability of mitochondria over a more extended period of time, we used photo-convertible mEos2 [20, 21] targeted to the mitochondrial matrix (mito-mEos2; Figure 3A–B). This allowed us to label a few mitochondria in distal portions of the axon and image at a much lower frequency (once every 15 minutes) for a longer period of time (12 hours), yet still determine unambiguously that the same mitochondria are present over extended periods of time. Semiautomated tracking of the photo-converted mitochondria (Figure 3C–

D) revealed that 75% of mitochondria remained within 10 microns of their original position over 12 hours thus demonstrating that most mitochondria remain immobile over long periods of time in mature cortical axons *in vitro* (Figure 3E, Movie S3).

Mitochondrial motility is low in distal layer 2/3 axons *in vivo*

Finally, we wanted to determine if the results we had obtained in mature cortical axons *in vitro* were recapitulated *in vivo* where the environment is much more complex than in a culture dish and obviously more physiological regarding metabolism, cell type diversity, and cellular architecture [22, 23]. To do this, we implemented an imaging paradigm for visualizing mitochondrial motility in distal layer 2/3 axons of cortical pyramidal neurons by *in vivo* 2-photon microscopy (Figure 4A). In short, mouse embryos were electroporated unilaterally *in utero* at embryonic day E15.5 (to target progenitors giving rise to layer 2/3 pyramidal neurons) with plasmids encoding mito-YFP and cytosolic tdTomato. (P)ostnatal day 10–12 or P23–24 mice were fitted with a cranial window and a head-fixing post for live imaging on a 2-photon microscope [24]. As shown in Figure 4B, we were able to find and image distal layer 2/3 axons filled with labeled mitochondria and tdTomato on the side contralateral to the electroporated hemisphere. We first performed live imaging on anesthetized mice at P10–12 and P29–30 (Figure 4C). Surprisingly even at the early developmental stage of P10–12, mitochondria are highly immobile with approximately 90% of mitochondria being stable for the entire imaging session (10–20 min; Figure 4D–E). Since different forms of anesthesia are known to affect mitochondrial function and therefore may affect mitochondrial dynamics [25–28], we performed imaging on awake behaving mice at P30–33 and P45 to demonstrate that anesthesia was not the reason for the lack of mitochondrial motility, (Figure 4C, Movie S4) and established again that > 90% of mitochondria were stationary over the entire imaging session (Figure 4D–E, ANOVA, p=0.1097). Recent advances in imaging and surgical techniques have begun to allow for the study of mitochondrial motility and function *in vivo*. Misgeld et al (2007) provided the first hint that mitochondrial motility is likely low *in vivo* when they showed in the sciatic nerve (PNS) of mice that ~ 90% of mitochondria are stationary both in slice preparations and *in vivo* [29]. In Rohon-Beard cells (PNS) of zebrafish, *in vivo* imaging of axonal mitochondria revealed a low percentage of moving mitochondria (between 1%–17%) which depended on the distance of the imaged segment from the cell body [30]. Finally, imaging of mitochondrial dynamics in mouse PNS axons of the saphenous nerves also revealed a high percentage of stationary mitochondria *in vivo* but found that high levels of neuronal activity significantly increased anterograde transport of mitochondria [31]. Coupled with other reports, our present results examining mammalian CNS cortical axons indicate that mitochondrial motility must be examined in mature *in vitro* and *in vivo* axons rather than immature *in vitro* culture models for inference of the molecular and cellular mechanisms underlying mitochondria dynamics and function in neurodegenerative diseases [32] (Table S1). An interesting example of this is with the mitochondrial anchoring protein Syntaphilin (SNPH). Loss of SNPH in short-term cultures from knockout mice show a dramatic increase in the number of motile mitochondria, but in slice cultures from four month old knockout mice the number of motile mitochondria is still very low suggesting other mechanisms for capturing/stabilizing mitochondria must be present [33, 34].

A recent report showing that mitochondrial transport is highly dynamic in axons of retinal ganglion cells *in vivo* [35] proposed that other current forms of imaging are too invasive and claim this is the reason for the low motility that is seen by other groups. However based on multiple recent reports using different axon subtypes and procedures [29–32, 34, 36, 37] (see Table S1), and also based on our present report showing that 21 days after window implantation mitochondrial motility is still very low in cortical axons of adult awake behaving mice, it is unlikely that inflammation or surgical procedure is the reason for these results. We believe that this discrepancy could be the result of a few different factors: (1) as mentioned above, distance from the cell body likely plays a role in the motility profile of the imaged mitochondria [30, 38], (2) based on this work and others, the motility profile is likely also influenced by the presence or absence of anchoring sites such as synaptic boutons and Nodes of Ranvier or in portions of the axons that are myelinated [10, 34], (3) it is likely that different types of neurons will have different motility profiles when considering the vast array of activity profiles that are found *in vivo* [10, 31, 34].

Finally, it is interesting to note that in dendrites of retinal ganglion cells examined in whole mount preparations, mitochondrial motility is also reduced as the neuron matures (~70% stationary mitochondria at P9 versus ~100% at P21) [37]. These authors nicely demonstrate that this is mitochondria specific (e.g. peroxisomes do not show this decreased in motility in adult stages) and that neither spontaneous nor sensory-evoked activity patterns regulate mitochondria dynamics.

Much of the literature examining mitochondrial dynamics in CNS axons has focused on the molecular mechanisms underlying their transport through microtubule-based motors such as dyneins and kinesins. Our results strongly argue that in the future, it will be important to improve our understanding of the mechanisms regulating mitochondrial immobilization, as well as the role that stationary mitochondria play at specific points along the axon. It is imperative that we devise the tools necessary to study mitochondria dynamics and function *in vivo*, in awake adult mice, over extended periods of time.

Experimental Procedures

Animals

All animals were handled according to protocols approved by the Institutional Animal Care and Use Committee (IACUC) at Columbia University. Time-pregnant CD1 females were purchased from Charles Rivers. Timed-pregnant hybrid F1 females were obtained by mating inbred 129/SvJ females, and C57Bl/6J males in house [4].

In utero cortical electroporation

In utero electroporations were performed as detailed in [4] with the exception that CD1 mice were used. See Supplemental Methods for more details.

Primary cortical culture and *ex utero* electroporation

Cortices from E15.5 CD1 mouse embryos were dissected followed by dissociation in cHBSS containing papain (Worthington) and DNAse I (100 μg/ml, Sigma) for 20 min at

37°C, washed three times and manually triturated in cHBSS supplemented with DNAse. Cells were plated at 7.5×10^4 cells per 35mm glass bottom dish (Mattek) coated with poly-D-lysine (1 mg/ml, Sigma) and cultured for 3–28 days in neurobasal medium supplemented with B27 (1X), FBS (2.5%), L-glutamine (2 mM). One third of the medium was changed every 5 days thereafter with non-FBS containing medium. *Ex utero* electroporation was performed as previously published in [4]. See Supplemental Methods for details and constructs.

Imaging

Imaging on dissociated neurons was performed between 3–28DIV on a Nikon Tie with either an EM-CCD camera (Andor) or A1-R confocal (Nikon). All *in vivo* imaging was performed on a custom 2-photon microscope (Bruker) in resonant galvo-mode and an ultra-fast pulsed laser tuned to 920nm (Coherent). See Supplemental Methods for detailed imaging methods.

Supplementary Material

Refer to Web version on PubMed Central for supplementary material.

Acknowledgments

References

1. Chen H, Chan DC. Mitochondrial dynamics--fusion, fission, movement, and mitophagy--in neurodegenerative diseases. Hum Mol Genet. 2009; 18:R169–176. [PubMed: 19808793]

2. Schon EA, Przedborski S. Mitochondria: the next (neurode)generation. Neuron. 2011; 70:1033–1053. [PubMed: 21689593]

3. Hirokawa N, Niwa S, Tanaka Y. Molecular motors in neurons: transport mechanisms and roles in brain function, development, and disease. Neuron. 2010; 68:610–638. [PubMed: 21092854]

4. Courchet J, Lewis TL Jr, Lee S, Courchet V, Liou DY, Aizawa S, Polleux F. Terminal axon branching is regulated by the LKB1-NUAK1 kinase pathway via presynaptic mitochondrial capture. Cell. 2013; 153:1510–1525. [PubMed: 23791179]

5. Spillane M, Ketschek A, Merianda TT, Twiss JL, Gallo G. Mitochondria coordinate sites of axon branching through localized intra-axonal protein synthesis. Cell Rep. 2013; 5:1564–1575. [PubMed: 24332852]

6. Wang X, Winter D, Ashrafi G, Schlehe J, Wong YL, Selkoe D, Rice S, Steen J, LaVoie MJ, Schwarz TL. PINK1 and Parkin target Miro for phosphorylation and degradation to arrest mitochondrial motility. Cell. 2011; 147:893–906. [PubMed: 22078885]

7. Brickley K, Stephenson FA. Trafficking kinesin protein (TRAK)-mediated transport of mitochondria in axons of hippocampal neurons. J Biol Chem. 2011; 286:18079–18092. [PubMed: 21454691]

8. Wang X, Schwarz TL. The mechanism of Ca2+-dependent regulation of kinesin-mediated mitochondrial motility. Cell. 2009; 136:163–174. [PubMed: 19135897]

9. Vossel KA, Zhang K, Brodbeck J, Daub AC, Sharma P, Finkbeiner S, Cui B, Mucke L. Tau reduction prevents Abeta-induced defects in axonal transport. Science. 2010; 330:198. [PubMed: 20829454]

10. Obashi K, Okabe S. Regulation of mitochondrial dynamics and distribution by synapse position and neuronal activity in the axon. Eur J Neurosci. 2013; 38:2350–2363. [PubMed: 23725294]

11. Ashrafi G, Schlehe JS, LaVoie MJ, Schwarz TL. Mitophagy of damaged mitochondria occurs locally in distal neuronal axons and requires PINK1 and Parkin. J Cell Biol. 2014; 206:655–670. [PubMed: 25154397]

12. Maday S, Holzbaur EL. Autophagosome biogenesis in primary neurons follows an ordered and spatially regulated pathway. Dev Cell. 2014; 30:71–85. [PubMed: 25026034]

13. Maday S, Wallace KE, Holzbaur EL. Autophagosomes initiate distally and mature during transport toward the cell soma in primary neurons. J Cell Biol. 2012; 196:407–417. [PubMed: 22331844]

14. Verburg J, Hollenbeck PJ. Mitochondrial membrane potential in axons increases with local nerve growth factor or semaphorin signaling. J Neurosci. 2008; 28:8306–8315. [PubMed: 18701693]

15. Gazit N, Vertkin I, Shapira I, Helm M, Slomowitz E, Sheiba M, Mor Y, Rizzoli S, Slutsky I. IGF-1 Receptor Differentially Regulates Spontaneous and Evoked Transmission via Mitochondria at Hippocampal Synapses. Neuron. 2016; 89:583–597. [PubMed: 26804996]

16. Kwon SK, Sando R 3rd, Lewis TL, Hirabayashi Y, Maximov A, Polleux F. LKB1 Regulates Mitochondria-Dependent Presynaptic Calcium Clearance and Neurotransmitter Release Properties at Excitatory Synapses along Cortical Axons. PLoS Biol. 2016; 14:e1002516. [PubMed: 27429220]

17. Chang KT, Niescier RF, Min KT. Mitochondrial matrix Ca2+ as an intrinsic signal regulating mitochondrial motility in axons. Proc Natl Acad Sci U S A. 2011; 108:15456–15461. [PubMed: 21876166]

18. MacAskill AF, Brickley K, Stephenson FA, Kittler JT. GTPase dependent recruitment of Grif-1 by Miro1 regulates mitochondrial trafficking in hippocampal neurons. Mol Cell Neurosci. 2009; 40:301–312. [PubMed: 19103291]

19. Saotome M, Safiulina D, Szabadkai G, Das S, Fransson A, Aspenstrom P, Rizzuto R, Hajnoczky G. Bidirectional Ca2+-dependent control of mitochondrial dynamics by the Miro GTPase. Proc Natl Acad Sci U S A. 2008; 105:20728–20733. [PubMed: 19098100]

20. Owens GC, Walcott EC. Extensive fusion of mitochondria in spinal cord motor neurons. PLoS One. 2012; 7:e38435. [PubMed: 22701641]

21. McKinney SA, Murphy CS, Hazelwood KL, Davidson MW, Looger LL. A bright and photostable photoconvertible fluorescent protein. Nat Methods. 2009; 6:131–133. [PubMed: 19169260]

22. Polleux F, Giger RJ, Ginty DD, Kolodkin AL, Ghosh A. Patterning of cortical efferent projections by semaphorin-neuropilin interactions. Science. 1998; 282:1904–1906. [PubMed: 9836643]

23. Polleux F, Morrow T, Ghosh A. Semaphorin 3A is a chemoattractant for cortical apical dendrites. Nature. 2000; 404:567–573. [PubMed: 10766232]

24. Kaifosh P, Lovett-Barron M, Turi GF, Reardon TR, Losonczy A. Septo-hippocampal GABAergic signaling across multiple modalities in awake mice. Nat Neurosci. 2013; 16:1182–1184. [PubMed: 23912949]

25. Hara K, Harris RA. The anesthetic mechanism of urethane: the effects on neurotransmitter-gated ion channels. Anesth Analg. 2002; 94:313–318. table of contents. [PubMed: 11812690]

26. Zaugg M, Lucchinetti E, Spahn DR, Pasch T, Garcia C, Schaub MC. Differential effects of anesthetics on mitochondrial K(ATP) channel activity and cardiomyocyte protection. Anesthesiology. 2002; 97:15–23. [PubMed: 12131099]

27. de Oliveira L, Fraga DB, De Luca RD, Canever L, Ghedim FV, Matos MP, Streck EL, Quevedo J, Zugno AI. Behavioral changes and mitochondrial dysfunction in a rat model of schizophrenia induced by ketamine. Metab Brain Dis. 2011; 26:69–77. [PubMed: 21331561]

28. Sanchez V, Feinstein SD, Lunardi N, Joksovic PM, Boscolo A, Todorovic SM, Jevtovic-Todorovic V. General Anesthesia Causes Long-term Impairment of Mitochondrial Morphogenesis and Synaptic Transmission in Developing Rat Brain. Anesthesiology. 2011; 115:992–1002. [PubMed: 21909020]

29. Misgeld T, Kerschensteiner M, Bareyre FM, Burgess RW, Lichtman JW. Imaging axonal transport of mitochondria in vivo. Nat Methods. 2007; 4:559–561. [PubMed: 17558414]

30. Plucinska G, Paquet D, Hruscha A, Godinho L, Haass C, Schmid B, Misgeld T. In vivo imaging of disease-related mitochondrial dynamics in a vertebrate model system. J Neurosci. 2012; 32:16203–16212. [PubMed: 23152604]

31. Sajic M, Mastrolia V, Lee CY, Trigo D, Sadeghian M, Mosley AJ, Gregson NA, Duchen MR, Smith KJ. Impulse conduction increases mitochondrial transport in adult mammalian peripheral nerves in vivo. PLoS Biol. 2013; 11:e1001754. [PubMed: 24391474]

32. Sorbara CD, Wagner NE, Ladwig A, Nikic I, Merkler D, Kleele T, Marinkovic P, Naumann R, Godinho L, Bareyre FM, et al. Pervasive axonal transport deficits in multiple sclerosis models. Neuron. 2014; 84:1183–1190. [PubMed: 25433639]

33. Kang JS, Tian JH, Pan PY, Zald P, Li C, Deng C, Sheng ZH. Docking of axonal mitochondria by syntaphilin controls their mobility and affects short-term facilitation. Cell. 2008; 132:137–148. [PubMed: 18191227]

34. Ohno N, Kidd GJ, Mahad D, Kiryu-Seo S, Avishai A, Komuro H, Trapp BD. Myelination and axonal electrical activity modulate the distribution and motility of mitochondria at CNS nodes of Ranvier. J Neurosci. 2011; 31:7249–7258. [PubMed: 21593309]

35. Takihara Y, Inatani M, Eto K, Inoue T, Kreymerman A, Miyake S, Ueno S, Nagaya M, Nakanishi A, Iwao K, et al. In vivo imaging of axonal transport of mitochondria in the diseased and aged mammalian CNS. Proc Natl Acad Sci U S A. 2015; 112:10515–10520. [PubMed: 26240337]

36. Jackson JG, O'Donnell JC, Takano H, Coulter DA, Robinson MB. Neuronal activity and glutamate uptake decrease mitochondrial mobility in astrocytes and position mitochondria near glutamate transporters. J Neurosci. 2014; 34:1613–1624. [PubMed: 24478345]

37. Faits MC, Zhang C, Soto F, Kerschensteiner D. Dendritic mitochondria reach stable positions during circuit development. Elife. 2016; 5

38. Shidara Y, Hollenbeck PJ. Defects in mitochondrial axonal transport and membrane potential without increased reactive oxygen species production in a Drosophila model of Friedreich ataxia. J Neurosci. 2010; 30:11369–11378. [PubMed: 20739558]

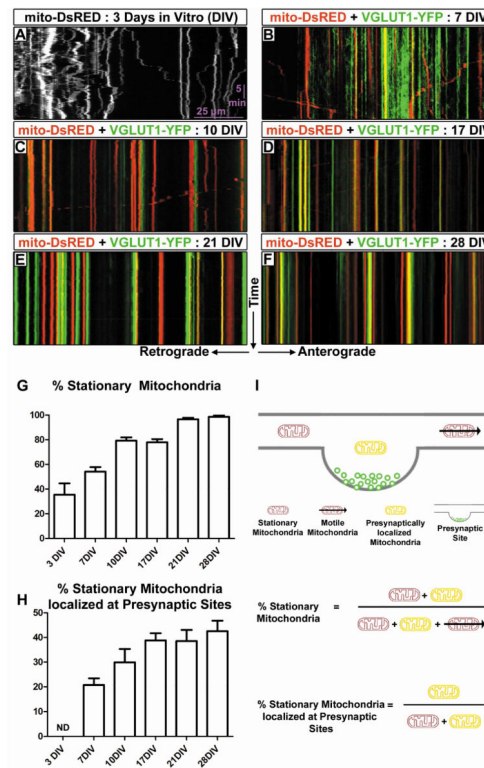**Figure 1. Mitochondrial motility decreases as the axon matures *in vitro***

(**A**) Representative kymograph of mitochondria in the axon of a cultured cortical neuron at 3DIV. On average only 35% of mitochondria are stationary. Stationary mitochondria are those mitochondria which move less than 5μm from the point of origin over the 30 minutes of timelapse microscopy. The y-axis represents time, while the x-axis represents direction of transport. Timelapse videos were acquired at 0.1fps for 30 minutes. (**B–F**) Representative dual color kymographs of mitochondria (red) and VGLUT1 (green) in the axons of cultured cortical neurons at 7DIV, 10DIV, 17DIV, 21DIV and 28DIV respectively. (**G**) Graph demonstrating the percent of stationary axonal mitochondria at various days in culture. Axonal development coincides with an increase in the number of stationary mitochondria. (**H**) Graph demonstrating the percent of stationary mitochondria which are localized at presynaptic sites. Localization is defined as overlap with the same stationary VGLUT1 puncta for the entire 30 minutes of the timelapse. The decrease in axonal mitochondrial motility coincides with increased localization of mitochondria at presynaptic sites. (**I**) Schematic representation of the parameters calculated in G and H. N = 8, 27, 15, 17, 17 and 18 axon segments at 3, 7, 10, 17, 21 and 28 DIV respectively. Statistical test: Anova with Dunns multiple comparison test. All error bars represent standard error of the mean. See also Figure S1, Movie S1 and Table S1.
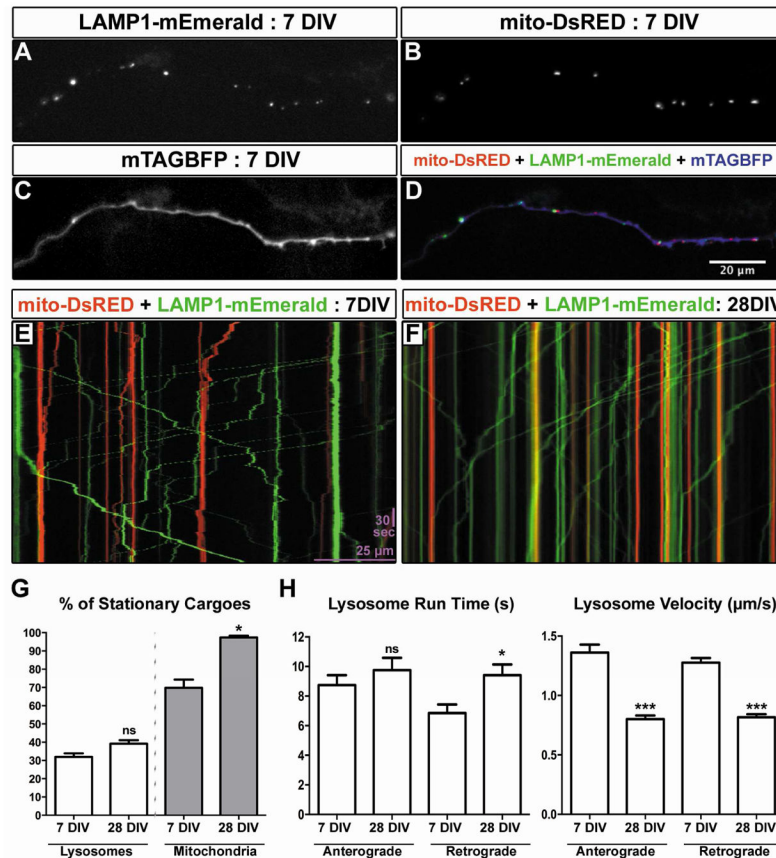
Figure 2. Lysosome motility does not decrease during axonal maturation *in vitro*
(**A–D**) Representative images of a 7DIV axon expressing LAMP1-mEmerald (A), mitoDsRED (B) and mTAGBFP (C) after ex utero electroporation at E15.5. (**E**) Representative kymograph of mitochondria (red) and LAMP1 (green) in the axon of a cultured cortical neuron at 7DIV. (**F**) Representative kymograph of mitochondria (red) and LAMP1 (green) in the axon of a cultured cortical neuron at 28DIV. (**G**) Graph comparing the percent of stationary lysosomes to the percent of stationary mitochondria at 7 and 28DIV. The number of motile axonal lysosomes doesn't change significantly between 7 and 28DIV, while the percentage of stationary axonal mitochondria increases at 28DIV. (**H**) Graphs comparing lysosomal run time and velocity of anterograde and retrograde transport at 7 and 28DIV. While run time slightly increases for motile lysosomes, the velocity is much less at 28DIV. N = 18 axon segments at 7DIV and 26 axon segments at 28DIV. Statistical test: ANOVA with Dunns multiple comparison test. All error bars represent standard error of the mean. See also Movie S2.
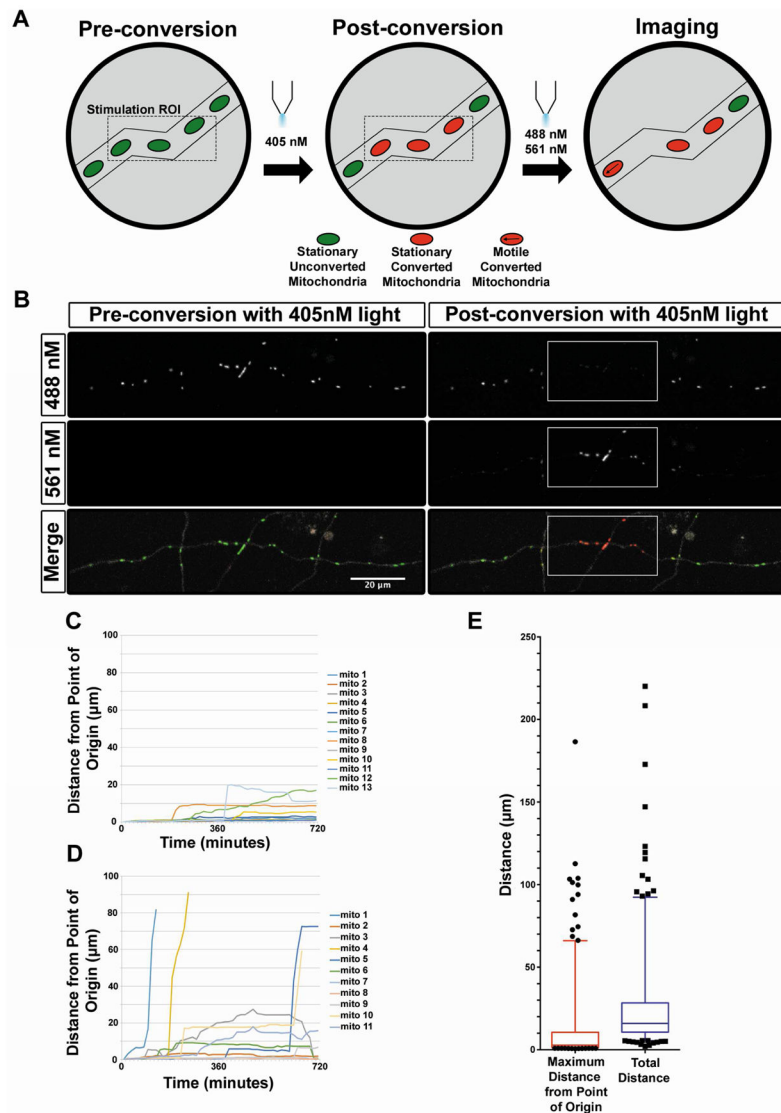
Figure 3. Long-term time lapse microscopy with photo-convertible mEos2 reveals highly stable mitochondria in mature axons *in vitro*

(**A**) Schematic representation of long-term time lapse imaging setup. Upon photo-conversion of mito-mEos2, all mitochondria within a short segment of the axon (30 to 50 μm) were converted from green to red fluorescence. Timelapse imaging was then performed every 15 minutes for 12 hours for both the red and green forms of mEos2. (**B**) A 28 DIV cortical axon expressing mito-mEos2 before and after photo-conversion by 405nm light. White boxes label the ROI for 405nm stimulation. (**C**) Graph of individual photo-converted mitochondrial motility in a representative axon with low mitochondrial motility. (**D**) Graph of individual photo-converted mitochondrial motility in an axon with higher mitochondrial motility. (**E**) Quantification of maximum distance from the point of origin and total distance moved for each mitochondria tracked over 12 hours revealing that 75% of mitochondria moved 10 microns or less from their original positions. N = 261 mitochondria from 23 axons (4 independent cultures). Data in E is represented as 5–95% whisker box plots with 25th, 50th,

and 75th percentiles shown by the lower, middle and top of the boxes. Outliers are represented by black dots. See also Movie S3.
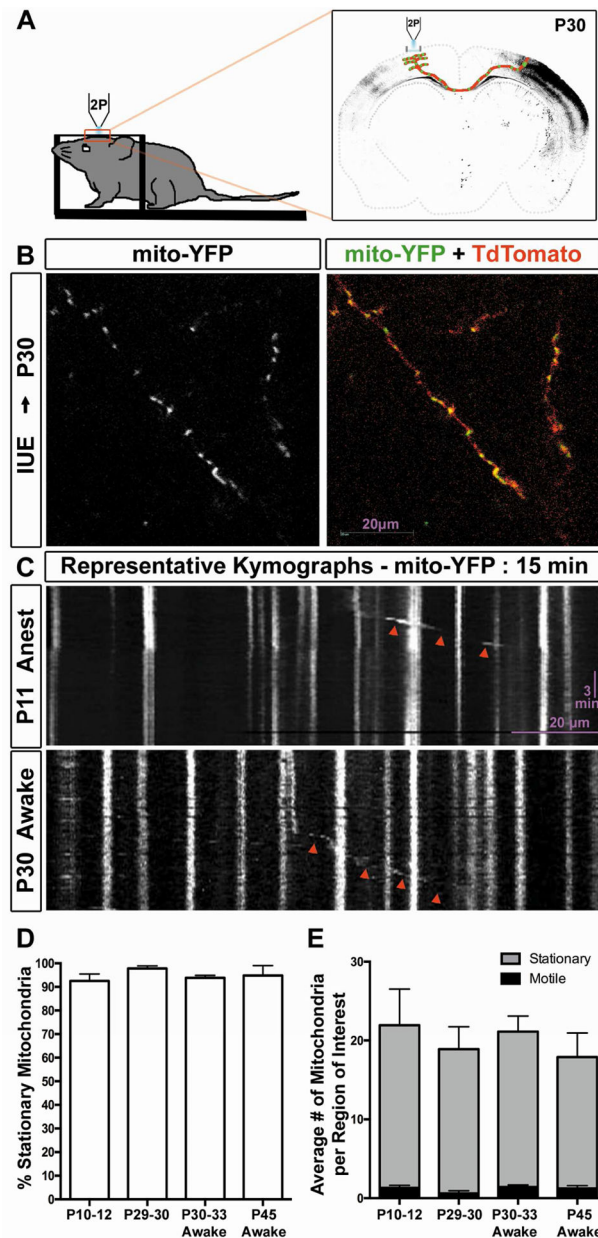
Figure 4. Mitochondrial motility is remarkably low in distal layer 2/3 axons *in vivo*

(**A**) Schematic representation of the imaging setup used to image axonal mitochondria in layer 2/3 pyramidal axon collaterals via 2-photon microscopy after *in utero* electroporation at E15.5. (**B**). Representative imaging field from the contralateral hemisphere at postnatal day 30. The left panel displays mitochondria labeled with YFP, while the right panel is the merge of mito-YFP and tdTomato to visualize the axon collaterals. (**C**) Representative kymographs of mitochondria labeled with YFP and imaged over a period of 15 minutes at 0.1fps. Top panel represents mitochondrial motility at P11, while the bottom panel represents mitochondrial motility at P30. Red arrowheads point to motile mitochondria. (**D**) Graph demonstrating the percent of stationary mitochondria under four different conditions:

P10–12 anesthetized mice, P29–30 anesthetized mice, P30–33 awake mice and P45 awake mice. Mitochondrial motility is remarkably low in all four conditions. (**E**) Graph comparing the number of motile and stationary mitochondria in the four conditions tested. n=17, 11, 24, 9 regions of interest from 6, 3, 6, 2 mice at P10–12 (anesthetized), P29–30 (anesthetized), P30–33 (awake), and P45 (awake) respectively. Statistical test: Anova with Dunns multiple comparison test. All error bars represent standard error of the mean. See also Movie S4.